PLASMA DYNAMICS

XIV. PLASMA PHYSICS*

Prof. S. C. Brown
Prof. G. Bekefi
Prof. K. U. Ingard
Prof. D. R. Whitehouse
Dr. J. C. Ingraham
Dr. G. Lampis
M. L. Andrews
F. X. Crist
J. K. Domen
E. W. Fitzgerald, Jr.
G. A. Garosi
K. W. Gentle
E. V. George
W. H. Glenn, Jr.
E. B. Hooper, Jr.
P. W. Jameson
R. L. Kronquist
D. T. Llewellyn-Jones
E. M. Mattison
J. J. McCarthy
W. J. Mulligan
J. J. Nolan, Jr.
L. D. Pleasance
G. L. Rogoff
D. W. Swain
F. Y-F. Tse
B. L. Wright

RESEARCH OBJECTIVES

The aim of this group continues to be the study of the fundamental properties of plasmas. We have been placing particular emphasis on plasmas in magnetic fields, plasmas of high percentage ionization at low pressures, and most recently on a plasma showing turbulence in high-speed flow.

We are also studying ways of determining the characteristics of plasmas by means of very far infrared optics in the wavelength range 0.1-1 mm, and by means of optical lasers.

The infrared diagnostic techniques are closely correlated with our continued effort to improve the more standard microwave methods. Most of our microwave techniques at the present time involve the study of microwave radiation from plasmas, with and without magnetic fields.

Theoretical work has concentrated on the study of waves in plasma, turbulence in flowing gases, and the statistical nature of plasmas.

S. C. Brown

A. REFLECTION OF GUIDED WAVES FROM A PLASMA COLUMN IN AN AXIAL MAGNETIC FIELD

In the course of the development of a microwave system for measuring cyclotron emission from an argon discharge, a study was made of the reflection of guided waves

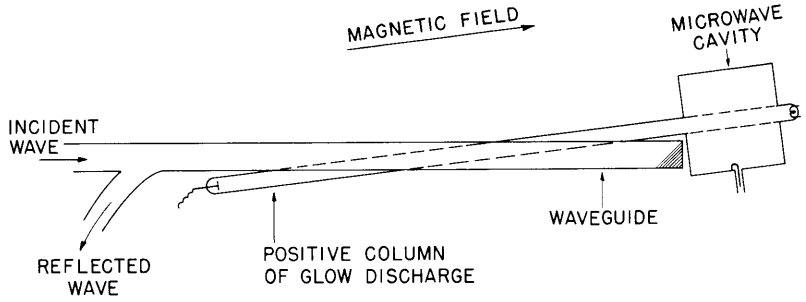

Fig. XIV-1. Diagram of the apparatus.

*This work was supported in part by the United States Atomic Energy Commission (Contract AT(30-1)-1842).

from an axially magnetized plasma column. Figure XIV-1 illustrates the configuration in question: a discharge tube, 1 inch in diameter, was inserted at an angle of 8° in a section of S-band waveguide terminated by a matched load. A directional coupler and crystal detector monitored the total reflected power. Observations were carried out in the afterglow of the pulsed DC discharge, the density decay being measured by the microwave cavity. At an argon pressure of approximately 2 Torr, a 90-ma pulse provided an initial electron density of 10^{11} cm^{-3}. The amount of reflected power was viewed during the density decay at values of the applied magnetic field ranging from zero to 2000 gauss.

The oscilloscope traces shown in Fig. XIV-2 illustrate the effects generally observed. All three have a time scale of 100 μsec/div and were triggered at the beginning of the

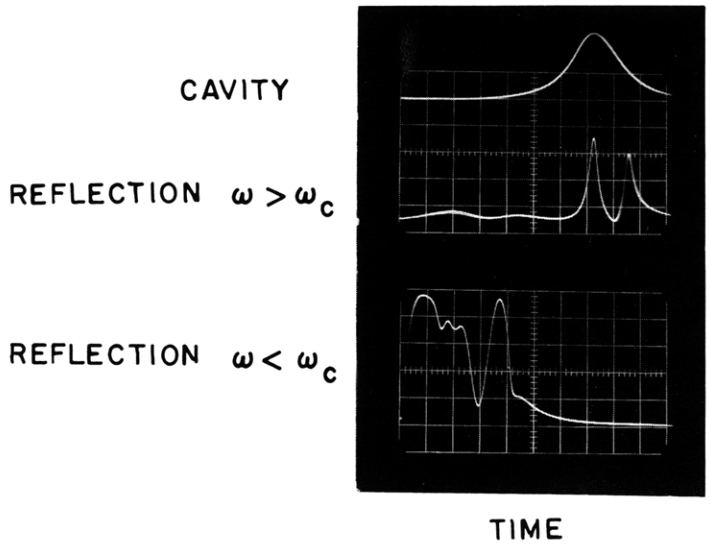

Fig. XIV-2. Oscilloscope traces showing cavity response and peaks in reflected power during the afterglow.

afterglow. The top trace shows the resonance response of the cavity that was used for density measurement. The middle curve indicates a double peak in reflection seen at magnetic fields whose cyclotron frequency is less than the frequency of the incident wave. For this sample, the applied field was zero and the height of the peaks represents reflection of approximately one-tenth of the incident power. As the applied magnetic field is increased, these peaks move outward in time (to lower electron densities), vanishing just before cyclotron resonance is reached. When the cyclotron frequency of the applied field exceeds the frequency of the incident wave, the power reflection in the afterglow jumps to around 50 per cent and several maxima and minima are observed, as illustrated

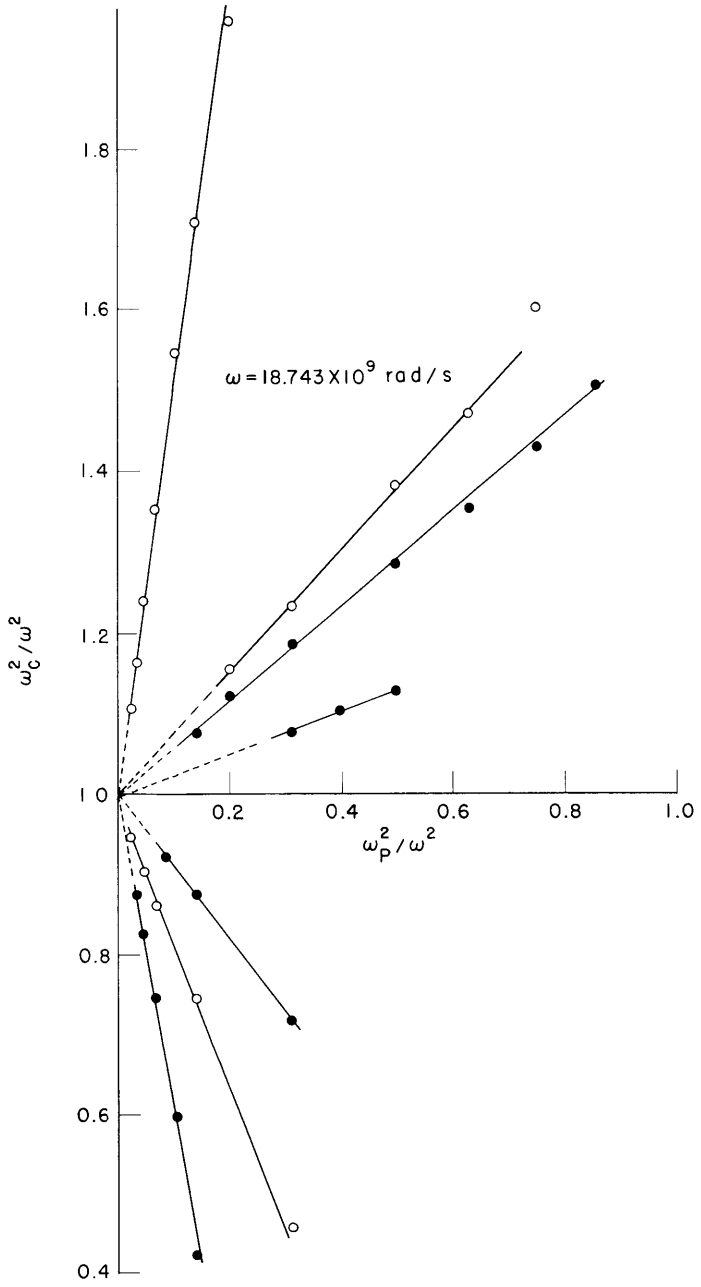

Fig. XIV-3. Loci of reflection maxima and minima at a fixed incident frequency.

by the lowest trace in Fig. XIV-2. As the magnetic field is increased further, this new pattern moves inward in time (to higher densities).

Over a wide range of gas pressures and electron temperatures it was seen that the positions of the maxima and minima depended only on electron density and magnetic field – a result that is consistent with the theory of electromagnetic waves in cold plasma. This dependence can be shown graphically by plotting the combinations of magnetic field and density at which a given maximum or minimum occurs. Such a plot is shown in Fig. XIV-3 for a fixed value of the angular frequency ω of the incident wave, with the average electron density in the tube and the magnetic field given in terms of the normalized variables ω_p^2/ω^2 and ω_c^2/ω^2. The small circles represent the loci of maxima in the reflected power, and the black dots give the loci of minima. The result is a series of fairly straight lines which, if extended to the limit of zero density, would intercept the vertical axis at $\omega_c^2/\omega^2 = 1$.

Variation of the incident frequency from 2500 Mc to 3750 Mc had the effect of changing the slopes of these lines in a smooth fashion. For instance, Fig. XIV-4 illustrates the progress in the ω_c^2, ω_p^2-plane of a single minimum that maintained its identity

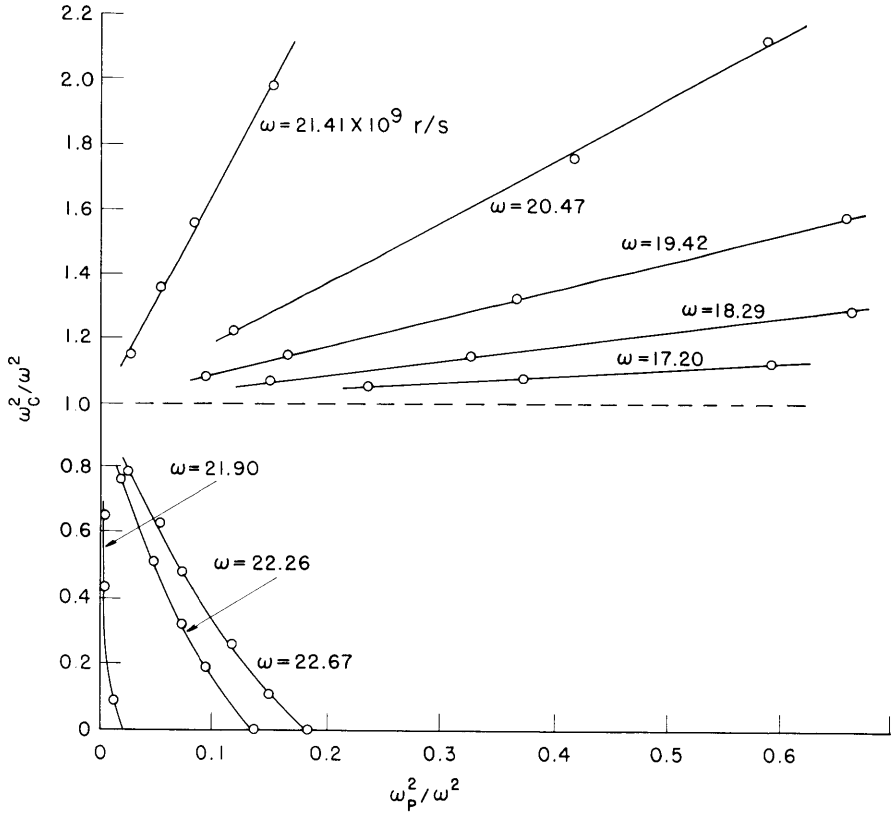

Fig. XIV-4. Loci of a given reflection minimum at various incident frequencies.

as ω, the angular frequency of incident wave, was varied over the range indicated. At a low frequency the trace emerges just above the line $\omega_c^2/\omega^2 = 1$ and as ω increases, it rotates continuously up to the vertical axis. At this point there is an abrupt flip down into the region of $\omega_c < \omega$, and the reflection minimum appears as an effect which can be observed at zero magnetic field.

The qualitative explanation of these observed variations in reflected power is that they arise from interference of the guided waves reflected off the front and back faces of the plasma column. For a section of waveguide filled uniformly over a finite length, L, with magnetized plasma, the criterion for a maximum or minimum in the reflected power is that L corresponds to some definite number of wavelengths in the direction parallel to the waveguide. In other words, if $k_z(\omega, \omega_p, \omega_c)$ is the wave number along the waveguide, the loci traced by a given reflection maximum is a curve along which k_z is constant. Preliminary examination of the boundary value problem for a cold plasma indicates that the dependence of k_z on ω, ω_p, and ω_c is strongly related to the behavior of n_r, the index of refraction of right circularly polarized waves, given by

$$n_r^2 = 1 - \frac{\omega_p^2/\omega}{\omega - \omega_c}.$$

Lines of n_r = constant in the ω_p^2, ω_c^2-plane all intersect at $\omega = \omega_c$, $\omega_p = 0$ and undergo a transition from the lower to the upper part of the plane as n_r passes through one. Thus if k_z is a continuous function of ωn_r, this same transition will appear for a line of constant k_z as ω is varied.

The results for all of the maxima and minima studied are presented in Fig. XIV-5. Here, for convenience, the inverse of the slopes of lines traced in the ω_p^2, ω_c^2-plane is plotted as a function of ω. Maxima and minima are represented by the small circles and black dots, respectively. The three points at which the curves intercept the horizontal axis represent transitions from the upper to the lower part of the ω_p^2, ω_c^2-plane of lines of constant k_z. Of particular interest is the convergence of the curves at these intercepts. The horizontal axis represents the empty-waveguide solutions. As magnetized plasma is added, each solution is split into two separate modes, presumably with different dispersion relations between k_z and ω. This is not surprising because in the latter case, the wave equation is of fourth order and two distinct transverse wave numbers are allowed. In the experiment, the splitting did not completely disappear at zero magnetic field (see Fig. XIV-2) but this could be due to a slight geometrical asymmetry.

An additional effect, which deserves mention, has been observed in the reflection characteristics. As well as the strong interference effects just discussed, some much fainter dips were seen in the reflected power. These likewise depend on electron density

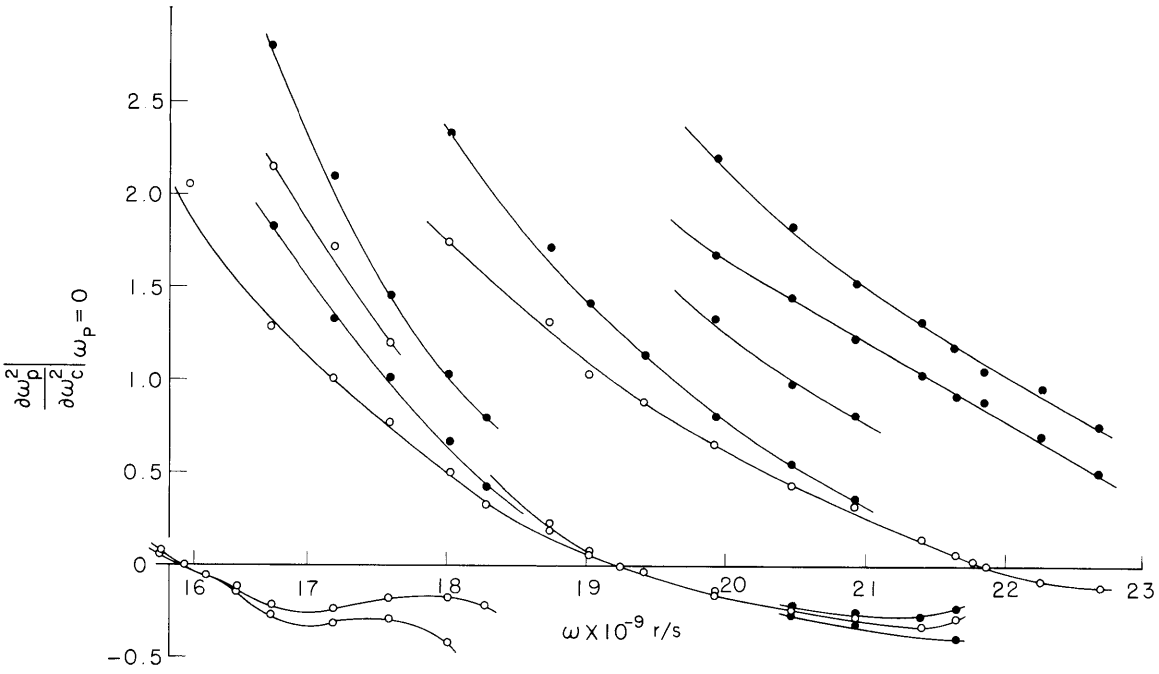

Fig. XIV-5. Inverse of the slopes of lines traced in the ω_p^2, ω_c^2-plane as a function of the incident frequency.

and magnetic field, but the loci, when plotted, form straight lines intercepting the vertical ω_c^2/ω^2-axis not at 1.00 but at 1.07. It is possible that this effect arises from the excitation of higher order waveguide modes that are not cut off in the plasma-filled section.

The equations governing the propagation of guided waves in a cold plasma have been given by Allis, Buchsbaum, and Bers,[1] but it would be difficult to obtain an exact solution for the configuration in question. Agreement with the theory is being sought in various limiting cases in order to understand more fully the general characteristics of the dispersion relation.

B. L. Wright

References

1. W. P. Allis, S. J. Buchsbaum, and A. Bers, Waves in Anisotropic Plasmas (The M. I. T. Press, Cambridge, Mass., 1963).

B. RF ABSORPTION BY A PLASMA NEAR THE ION CYCLOTRON HARMONICS

A system for the investigation of ion cyclotron resonance in a low-pressure arc has been described previously, and an experimental program for the determination of ion

energy-loss mechanisms in the plasma has been outlined.[1] In the course of this investigation a complex absorption spectrum has been observed in the range of magnetic fields for which

$$\frac{\omega}{5} \leqslant \Omega_i \leqslant \frac{\omega}{2},$$

where $\Omega_i = \frac{eB}{m_i}$ is the ion cyclotron frequency, and $\omega = 2\pi \times 10^6$ is the excitation frequency.

Some typical absorption spectra are described in this report; at present, a detailed interpretation of them must await further experimental investigation. Several hypotheses will be advanced as a guide for further work.

The plasma under investigation is a helium arc produced in a hollow-cathode discharge.[2] Helium gas is introduced into the vacuum chamber through both the cathode and a hollow tubular anode. A direct current of 3-40 amps is passed through the arc,

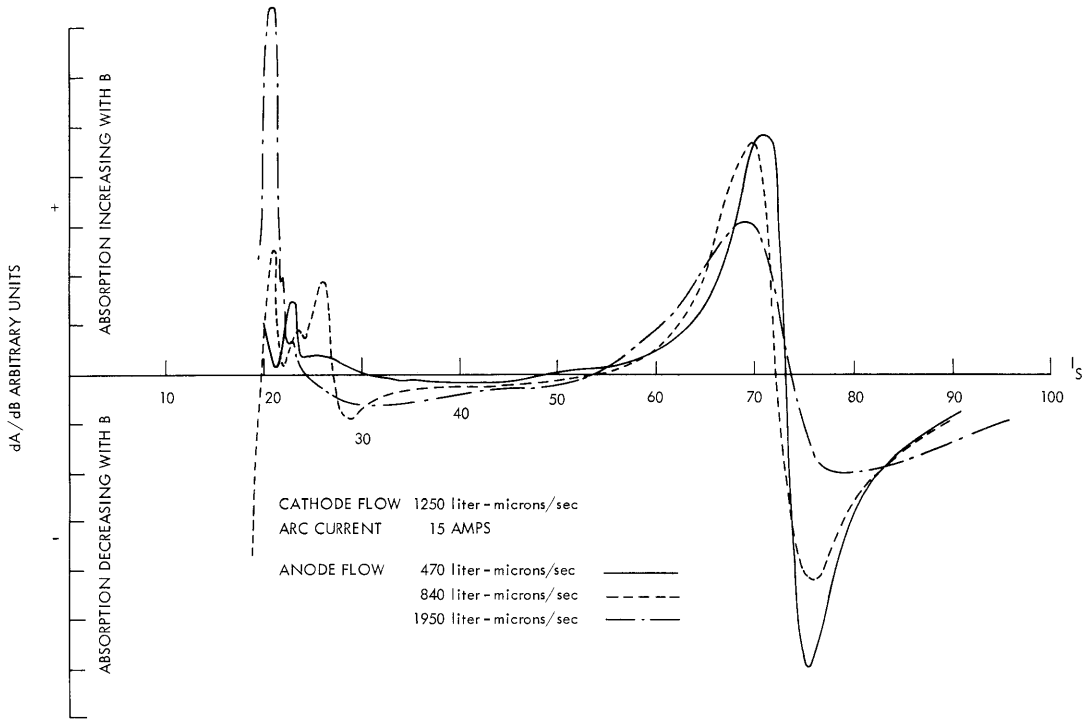

Fig. XIV-6. Plasma absorption spectra.

and produces ionization within the electrodes and in the chamber between them. The resulting plasma is confined by an axial magnetic field. The range of parameters of the arc is summarized as follows:

Axial magnetic field	0-4100 gauss
Solenoid driving current	I_s = 0-100 amps
Cathode (tantalum)	0.125 inch O.D. × 0.010 inch
Anode (copper)	0.375 inch I.D.
Cathode gas feed	$F_C = 0.5\text{-}2 \times 10^3$ liter-microns/sec
Anode gas feed	$F_A = 0.5\text{-}2 \times 10^3$ liter-microns/sec
Arc length	1 meter
Arc current	I_a = 3-40 amps
Arc voltage	40-80 volts
Ambient neutral pressure	$1\text{-}10 \times 10^{-3}$ torr
Plasma density on axis	$0.5\text{-}5 \times 10^{14}$ cm^{-3}

The plasma is surrounded by a periodic induction coil,[1,3] 30 cm long, with a 20-cm space period. The coil is the unknown element in an RF bridge operating at a frequency of 1 megacycle. The axial magnetic field is modulated at 100 cps by an additional winding surrounding the plasma. Through a system of synchronous detection the bridge produces DC signals proportional to dA/dB and dD/dB, where A and D are the plasma absorption and dispersion, respectively. These quantities may be investigated as functions of the arc current, gas flow, and magnetic field.

Figure XIV-6 shows some typical absorption spectra. The function plotted is dA/dB versus B with the gas feed as a parameter. For these three spectra the arc current was held constant at 15 amps. The sense of the measurements is such that with increasing $B(I_s)$, a zero crossing from above represents a maximum in the absorption and a zero crossing from below, a minimum.

The dominant feature of these spectra is the large peak in absorption at $\Omega_i = \omega$ which occurs for B = 2605 gauss, I_s = 72.5 amps. This is the cyclotron resonance of the He^+ ion. The other striking feature is the complicated structure in the region $20 < I_s < 30$ amps. This region is shown in detail in Fig. XIV-7 for constant arc current and variable flow. Figure XIV-8 shows the same region, but for constant flow and variable arc current. The behavior of the absorption in this region may be summarized qualitatively in the observation that the significant features of the spectra, insofar as they persist, move upward in magnetic field with increasing arc current and downward with increasing gas feed.

In order to compare the observed absorption spectra with theory, it is necessary to express the absorption as a function of the plasma density and temperature. An oscillating Langmuir probe was used to provide information on the radial distribution of the

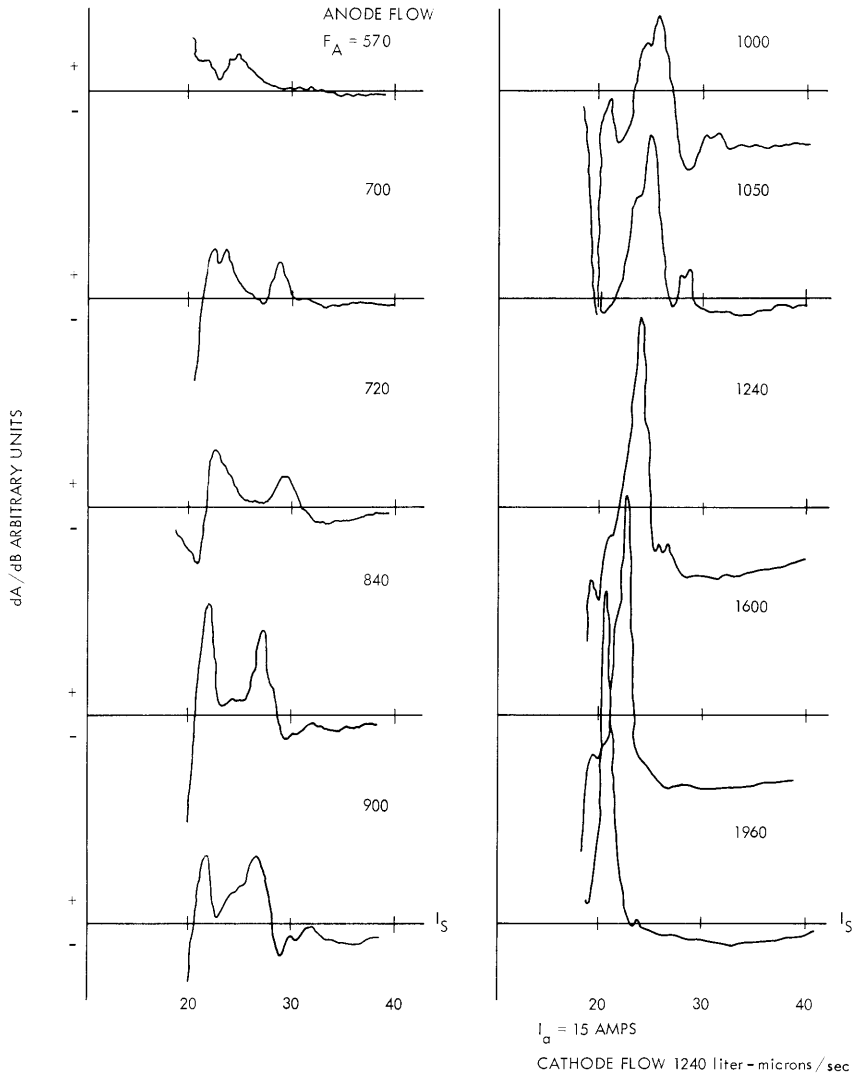

Fig. XIV-7. Plasma absorption spectra.

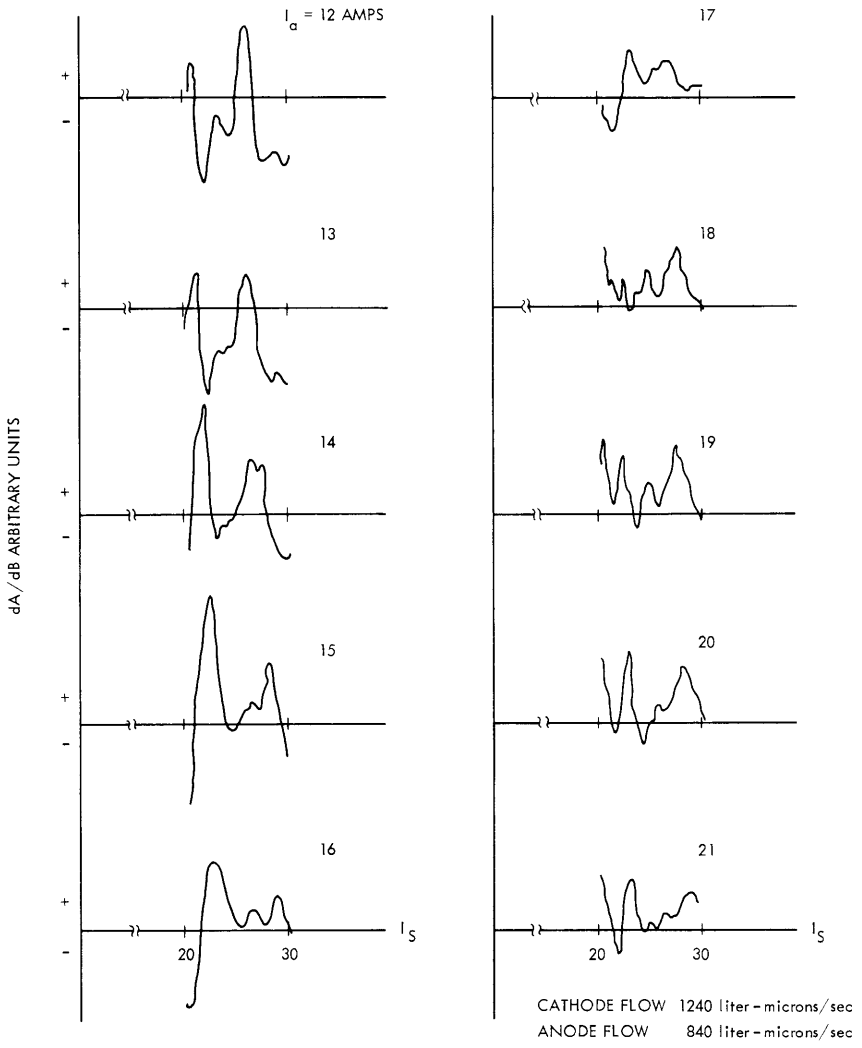

Fig. XIV-8. Plasma absorption spectra.

plasma parameters. The probe consists of a 0.030-inch tungsten rod which is insulated, except at the tip, by a thin-walled alumina tube. This probe is driven in and out of the plasma along a radius with a period of 6 seconds. With this probe, the ion saturation current may be obtained as a function of radius for different plasma conditions. It is not possible to measure the electron saturation current, since the theoretical value of several amperes would vaporize the probe in addition to perturbing the plasma. Profiles of the ion saturation have been taken over the range of parameters covered in Figs. XIV-7 and XIV-8. The profiles are generally bell-shaped curves with a half-width approximately equal to the anode diameter of 0.375 inch. Using the Bohm formula,[4] we have

$$I^+_{sat} = 0.4\, n_i e \sqrt{\frac{2eT_e}{M_i}},$$

and under the assumption of an electron temperature of 5 ev, we obtain the following values for the axial plasma density.

Anode Gas Feed

I_s (amps)	300	700	1240	1960	(liter-microns/sec)
20	0.89	1.0	1.33	1.67	10^{14} cm^{-3}
30	1.33	1.73	2.21	2.44	10^{14} cm^{-3}

The cathode gas feed was held constant at 1240 liter-microns/sec and the arc current was 15 amps in these measurements. The radial profile of ion saturation current is remarkably insensitive to the arc current, showing roughly a 10 per cent increase for currents of 10-20 amps.

A review of the possible modes of wave propagation in a plasma with the observed parameters indicates at least two possibilities, excitation of the Alfvén compressional wave or the electrostatic ion cyclotron harmonic wave. These possibilities are considered below. For a uniform cold plasma, the Alfvén compressional wave obeys the dispersion relation[3]

$$\frac{\omega^2}{\Omega_i^2} = \frac{k_z^2c^2 + \nu_m^2c^2}{\pi_i^2}\Omega_i^2 = \pi_i^2 \frac{\omega^2}{k_z^2c^2 + \nu_m^2c^2},$$

where π_i^2 is the ion plasma frequency, and k_z and ν_m are the axial and radial wave numbers. In the experimental situation, k_z and ω are fixed by the driving coil, and ν_m is determined by the radial boundary condition.

A coupling resonance with resulting increase in absorption should occur at the value of B for which the dispersion relation is satisfied. Specifically, the magnetic field for resonance should increase with increasing plasma density. From the probe data and the behavior of the absorption spectra, it may be seen that the magnetic field for which absorption maxima occur move downward with increasing density. It is unlikely, therefore, that the anomalous absorption is due to the excitation of Alfvén waves.

The electrostatic ion cyclotron waves have been considered by several authors.[3, 5] They are longitudinal in nature, that is, $\vec{k} \parallel \vec{E}$, and for minimum damping they propagate across the magnetic field $\vec{k} \perp \vec{B}_o$. For $k_z = 0$, a dispersion relation for these waves has been given by Stix[3]

$$\left[\frac{1}{\pi_i^2} + \frac{1}{\Omega_i\Omega_e}\right]\lambda_i = a(q, \lambda_i),$$

where

$$\lambda_i = \frac{k_x^2}{\Omega_i^2}\frac{\kappa T_i}{M_i} \sim \text{ion gyroradius/transverse wavelength}$$

$$q = \frac{\omega}{\Omega_i}.$$

The function α goes from $+\infty$ for $q = n + \epsilon$, n integral, to $-\infty$ for $q = (n+1) - \epsilon$. Consequently, this dispersion relation may be satisfied at at least one point between every $q = n$ and $q = n + 1$. Excitation of these waves could be responsible for the observed absorption but comparison with theory must await further experimental and theoretical analysis.

W. H. Glenn, Jr.

References

1. W. H. Glenn, Quarterly Progress Report No. 74, Research Laboratory of Electronics, M.I.T., July 15, 1964, pp. 69-74.

2. L. M. Lidsky, S. D. Rothleder, D. J. Rose, and S. Yoshikawa, J. Appl. Phys. 33, 2490 (1962).

3. T. Stix, Theory of Plasma Waves (McGraw Hill Book Company, Inc., New York, 1962).

4. D. Bohm, in The Characteristics of Electrical Discharges in Magnetic Fields, edited by A. Guthrie and R. K. Wakerling (McGraw Hill Book Company, Inc., New York, 1949).

5. F. W. Crawford, Report No. 1216, Microwave Research Laboratory, Stanford University, August 1964.

C. MICROWAVE MEASUREMENTS OF ELECTRON DIFFUSION IN A WEAKLY IONIZED FLOWING GAS

[This report is a revised version of a paper presented at the American Physical Society, Division of Plasma Physics Meeting, New York, November 4-7, 1964.]

As part of a general investigation of the influence of flow on the properties of a discharge in a weakly ionized gas, we have considered the enhanced diffusion that is to be expected if the gas flow is hydrodynamically turbulent. The effects of turbulent pipe flow had been briefly studied,[1] but the more intense turbulence that can be generated in jet flow produces more readily observed effects.[2]

Figure XIV-9 shows our experimental apparatus. The gas, either argon or helium, enters through the narrow tube, producing a turbulent jet that is convected downstream through the microwave cavity. The plasma is generated by pulsing the cavity in the

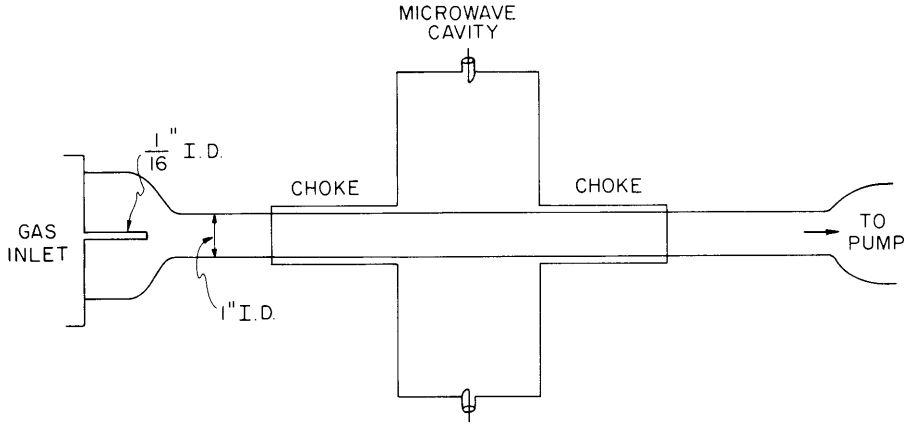

Fig. XIV-9. Experimental apparatus.

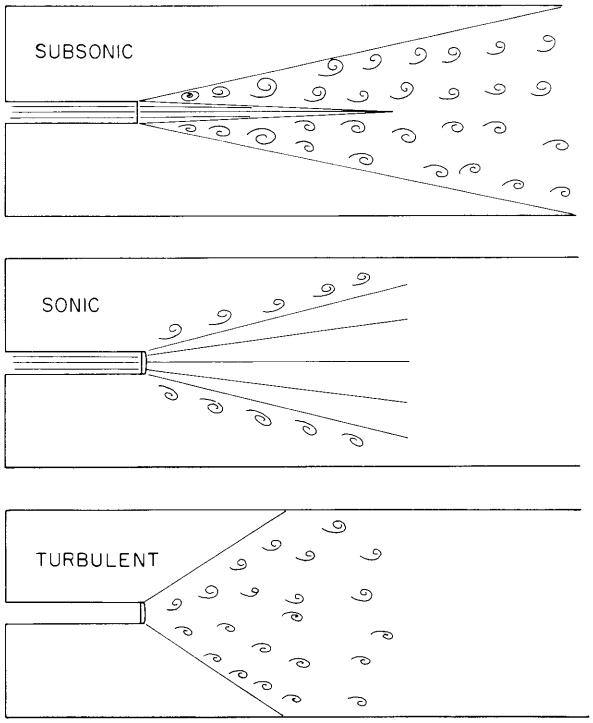

Fig. XIV-10. Schematic flow patterns.

TM_{020} mode at 2800 Mc with several watts of power at a 120-cycle repetition rate. The density in the afterglow can be determined by measuring the frequency shift of the TM_{011} resonance near 2400 Mc.

To interpret the experimental results, one must know the velocity profile created by the jet. Figure XIV-10 illustrates the three flow regimes. In the subsonic range, an ordinary jet with a laminar core is formed, surrounded by an expanding cone of turbulent gas. As the velocity in the jet tube increases, the turbulence becomes more intense. Further increases in flow cause the velocity to become sonic in the tube, and a shock front forms at the orfice. The flow behind the front is a divergent cone, within which the flow is laminar. The turbulent region is restricted to the boundary layer at the cone edge. Increasing the flow reduces the turbulent region somewhat, but when the Reynolds number of the flow in the jet tube exceeds the critical value of approximately 1800 and the flow entering the shock is turbulent already, the entire shock front becomes unstable. The full downstream flow then suddenly becomes strongly turbulent. The flow through the cavity tube is always below critical Reynolds number; this implies that the turbulence decays, but the turbulence is convected through before it is substantially attenuated.

Two types of experiment were designed to observe the effects of this turbulence. The most direct technique is to measure density as a function of time in the afterglow, from which a diffusion coefficient D is calculated. The presence of turbulence is indicated by an enhanced effective D. Alternatively, one can make quenching power measurements. Here, the pulse power is increased until breakdown occurs and then it is decreased. The power at which the discharge is extinguished is recorded. Quenching occurs when the cavity field is insufficient to raise the initial concentration to a stable discharge level during the pulse. It is therefore quite sensitive to diffusion, which governs the initial electron density. In both experiments, one observes the competition between turbulent diffusion and ambipolar diffusion for thermal electrons. Approximate theoretical calculations indicate that the two effects are of the same order of magnitude.

Typical results for quenching power measurements are shown in Figure XIV-11. The

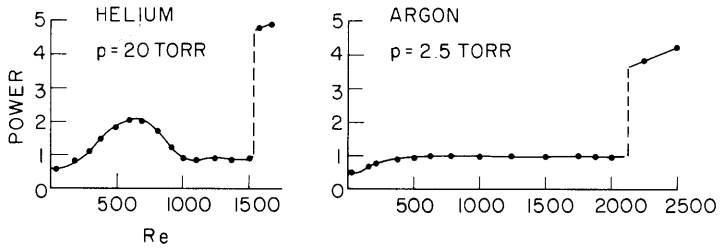

Fig. XIV-11. Quenching power vs flow.

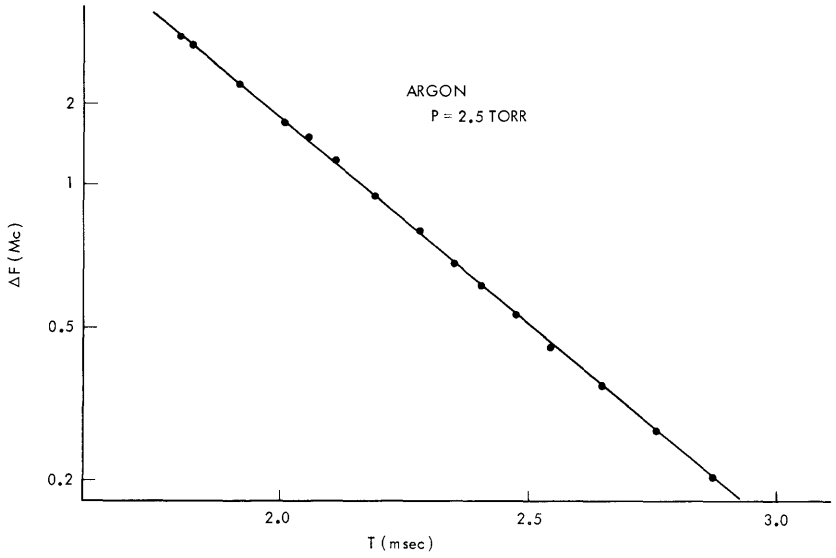

Fig. XIV-12. Density decay in afterglow.

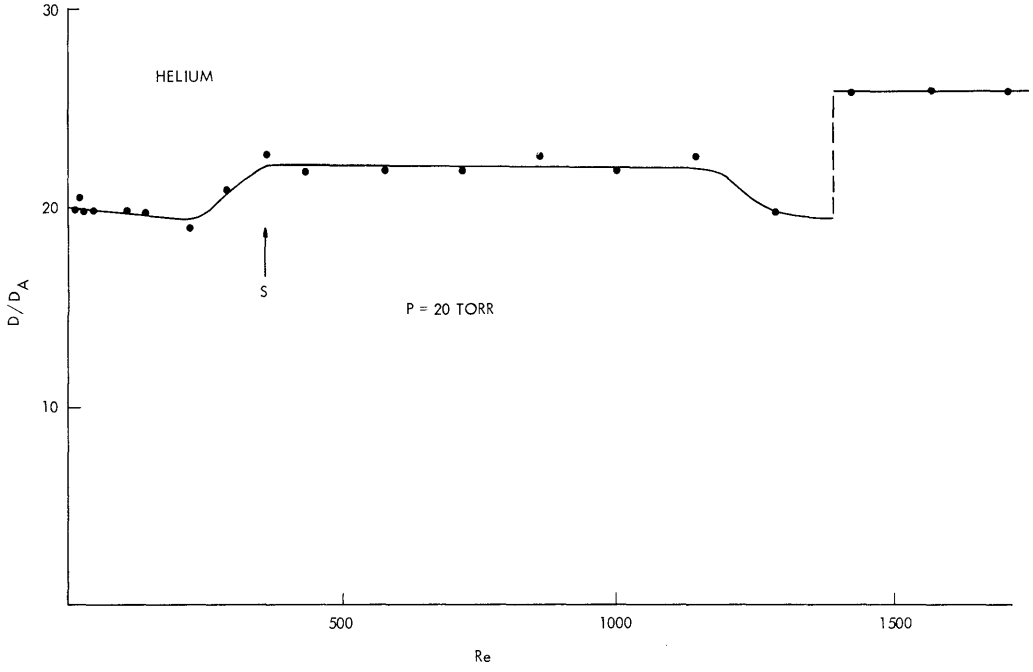

Fig. XIV-13. Effective diffusion vs flow.

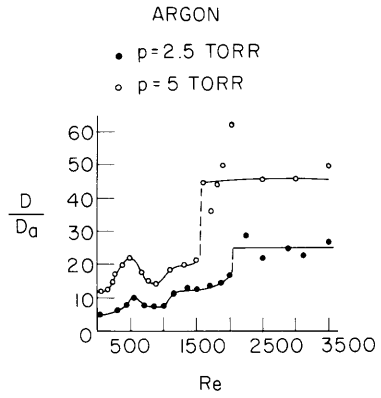

Fig. XIV-14. Effective diffusion vs flow (1-cm diameter).

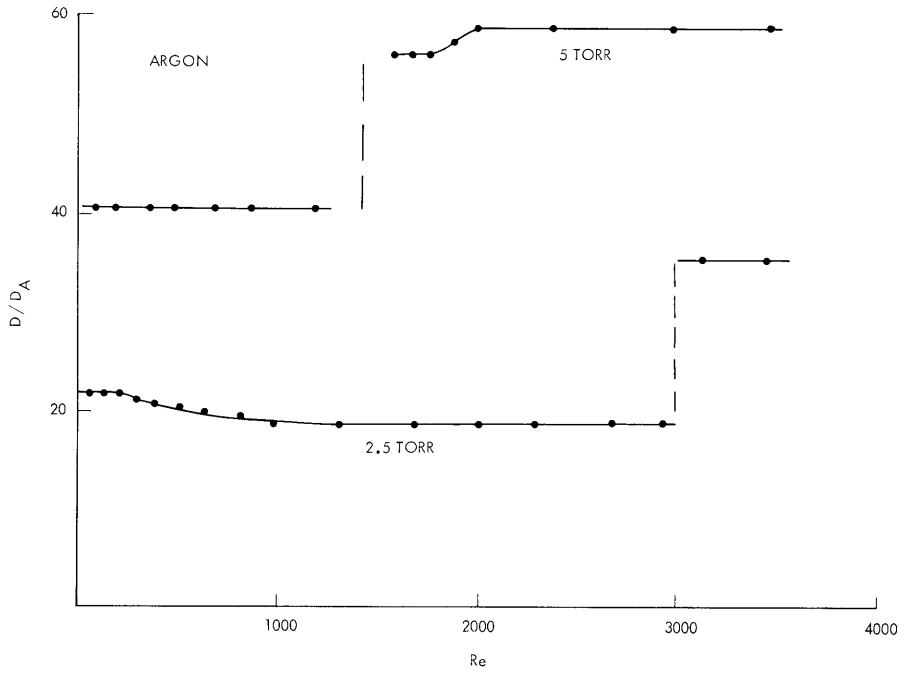

Fig. XIV-15. Effective diffusion vs flow (2.5-cm diameter).

quenching power follows the form predicted from the flow profile, with a sharp jump at the critical Reynolds number, when the entire stream breaks into strong turbulence. This onset of turbulence is also marked by the appearance of visual flickering in the discharge. Turbulence is particularly effective in raising quenching power because the occasional large fluctuations will quench the discharge, although they do not contribute much to the average diffusion.

The more significant measurement is that of effective diffusion from density decay. A typical semi-log plot of resonant frequency shift versus time in afterglow is shown in Fig. XIV-12. The good straight-line fit implies that electron loss is caused by a diffusion mechanism. In Fig. XIV-13 effective diffusion relative to ambipolar diffusion is plotted as a function of flow. The effective D increases as the jet becomes more intense and approaches sonic (point S), and jumps again when the whole stream turns turbulent, in agreement with qualitative predictions. The major puzzle has been the uniformly high values of diffusion; they are just ten times what one calculates for cold electrons. Recent measurements and calculations indicate that the 10 mw used for density diagnostics in the high-Q cavity may be sufficient to keep the electrons hot; this would explain the remarkably fast diffusion. Additional work on this hypothesis is in progress.

Similar measurements for argon are presented in Fig. XIV-14. These show the same features as helium. To guarantee that the large diffusion coefficients were independent of tube radius, the diameter of the glass tube through the cavity was changed from 1 cm to 2.5 cm (see Fig. XIV-15). In this larger tube, the turbulence decays more rapidly downstream. Only the turbulence from the unstable shock is sufficiently strong to reach the cavity with measurable intensity.

Considerably more work on the effect of turbulence in both jet and pipe flow is planned, particularly for explaining the large effective D even in the absence of flow. Until this problem is solved, theoretical calculations are impossible, and one cannot venture more than qualitative explanations of results based on the general features of the velocity profiles in the flow.

K. W. Gentle, G. A. Garosi, K. U. Ingard, G. Bekefi

References

1. K. W. Gentle, U. Ingard, and G. Bekefi, Nature 203, 1369 (1964).
2. W. B. Cottingham and S. J. Buchsbaum, Bull. Am. Phys. Soc. 8, 424 (1963).